Coupling the vortex dynamics with collective excitations in Bose-Einstein Condensate due modulation of the scattering length

R. P. Teles, V. S. Bagnato and F. E. A. dos Santos

Instituto de Física de São Carlos, USP, Caixa Postal 369,

13560-970 São Carlos, São Paulo, Brazil

Abstract

Here we made a study and implementation of suitable phases for a better description of physical systems using the variational method of variable parameters. Generally the condensate phases must be polynomials of degree equal to or greater than two. Thus taking a new appropriate phase was possible to calculate the collective modes of a condensate containing a single vortex along of the axial axis (cylindrical symmetry), as well as its free expansion. As result, a degeneracy was opened on each oscillatory mode already known, monopole (breathing) and quadrupole, being associated to vortex core oscillation in or out phase with respect to the axial radius. The high energetic mode just can be, effectively, seen using the modulation of scattering length.

I. INTRODUCTION

We are interested in observing the dynamics of a trapped condensate containing a line vortex at its center, i.e., in obtaining the collective oscillation modes of the system which couples the vortex core oscillation with the oscillation radii of the condensate. The interest in this problem came from the fact that these oscillations can be measured at laboratory when the atomic cloud is moved out its equilibrium point by using the Feshbach resonance in order to modulate the scattering length [1–5]. These oscillations are also studied in other physical systems such as: two-species condensates [6], BCS-BEC crossover [7–9], and Helium superfluid [10]. From the theoretical point of view we are interested on how the size of the vortex core oscillates with respect to the external dimensions of the cloud. A quadrupole mode occurs when the longitudinal and radial sizes of condensate oscillate out phase, being this one the mode with the smallest frequency of oscillation. The breathing mode requires more energy to be excited since the change of the density of atomic the cloud imposes a greater resistance to go out of balance than for quadrupole excitations [11, 12].

The dynamics of normal modes for a single vortex was studied on hydrodynamics models, which focus on movement of the vortex with respect to the mass center of the condensate [13–15]. This concept is also used in the case of multicomponent Bose-Einstein condensate [16].

Preliminary calculations using a variational calculation with a Gaussian Ansatz, which does not take into account the size of the vortex core [3, 6, 16, 17], shows a small shift in frequencies of the aforementioned modes (Figure 1). This shift has already been obtained via a hydrodynamic approximation by [12] and [18]. Thus we can expect that the frequency of the monopole (breathing) falls while the quadrupole frequency increases in the presence of the vortex.

To calculate this in a way more consistent with the physical reality which allows for the coupling between vortex core and radii of condensate, we use a Thomas-Fermi (TF) Ansatz [19],

$$\psi\left(\rho,\varphi,z,t\right) = A\left(t\right)\left[\frac{\rho^2}{\rho^2+\xi\left(t\right)^2}\right]^{\frac{1}{2}}e^{i\varphi}\sqrt{1-\frac{\rho^2}{R_\rho\left(t\right)^2}-\frac{z^2}{R_z\left(t\right)^2}}\exp\left[iB_\rho\left(t\right)\frac{\rho^2}{2}+iB_z\left(t\right)\frac{z^2}{2}\right],\tag{1}$$

and then calculate the equations of motion for the three parameters of the condensate. Following these calculations, the equations of motions were linearized. This procedure leads to imaginary frequencies which is not consistent with the stable configuration where a single vortex at center of the condensate. Therefore, we had the linearized equations given by
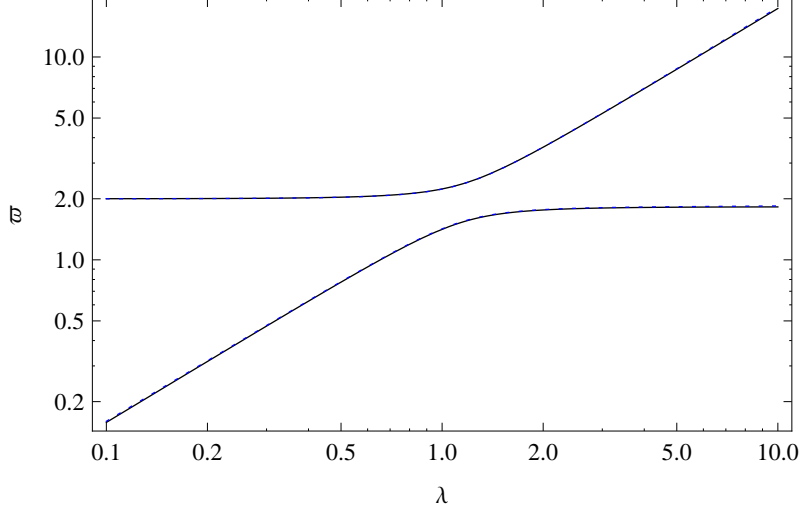
$$M\ddot{\delta}+V\delta=0,\tag{2}$$

Figure 1: The upper lines relate to the frequencies of the breathing mode as a function of the anisotropy of the harmonic potential (trap), whereas the lower lines represent the frequencies of the quadrupole mode. The solid (black) lines were used to the case of vortex-free TF-profile, and the dotted (blue) lines describe the Gaussian approximation for a profile with a single vortex. This approximation becomes poor above $\lambda \approx 1.5$ because the Gaussian line crosses the TF line for breathing mode, although it is unnoticeable on graph. Necessarily the presence of the vortex must decrease the frequency of breathing mode (does not agree with the region of oblate condensates), and increase the frequency of quadrupole mode (in agreement), being these the shift of the frequencies. Note that ϖ is normalized by the frequency of the radial direction ω_ρ.

and its frequency

$$\varpi^2 = \det\left(M^{-1}V\right) = \det M^{-1} \det V = \frac{\det V}{\det M}. \tag{3}$$

In order to obtain real frequencies and thus the expected stability. The both determinants above must necessarily be positive, since the sign of $\det V$ reflects the sign of the parameters which give us the radii of the cloud in the stationary situation. In the case of Ansatz (1) such conditions is not satisfied, $\det M^{-1} < 0$, which indicates that there is something wrong with Ansatz (1). As in the previous works [15, 16, 20, 21], the authors did not consider the size of the vortex core as a variational parameter, this problem did not appear. Indeed, the problem relies on the fact that the phase of wave function is incomplete. To solve this problem, we need to reconstruct the phase in this Ansatz.

In Section II, the necessary requirements for the wave function phase are discussed in order to give support to our variational method. The section III has the calculation that we drove from the Ansatz untill motion equations. The collective mode with coupling between vortex

and atomic cloud is obtained via linearization of the equations of motion, resulting on new collective oscillations (section IV). We showed that this excitation modes can be excited using the scattering length modulation at section V. The free expansion also has calculated to complement a preview work about expansion. Finishing the section VII contains the conclusions about our subject of study.

II. PHASE STUDY

We start with the Lagrangian,

$$\mathcal{L} = \frac{i\hbar}{2}\left(\psi^*\frac{\partial\psi}{\partial t} - \psi\frac{\partial\psi^*}{\partial t}\right) - \frac{\hbar^2}{2m}\left|\nabla\psi\right|^2 - V\left(\mathbf{r}\right)\left|\psi\right|^2 - \frac{g}{2}\left|\psi\right|^4 \tag{4}$$

whose extremilization leads to the GPE:

$$i\hbar\frac{\partial\psi}{\partial t} = \left[-\frac{\hbar^2}{2m}\nabla^2 + V\left(\mathbf{r}\right) + g\left|\psi\right|^2\right]\psi, \tag{5}$$

where $V\left(\mathbf{r}\right)$ is an external potential, and g the coupling contant. The complex field $\psi\left(\mathbf{r},t\right)$ can be write as density profile with a respective phase, as it follows:

$$\psi\left(\mathbf{r},t\right) = f\left(w_l,\mathbf{r}\right)e^{iS(\chi_l,\mathbf{r})}, \tag{6}$$

and

$$S\left(\chi_l,\mathbf{r}\right) = \sum_l \chi_l\phi_l(\mathbf{r}). \tag{7}$$

We denoted both, $w_l = w_l\left(t\right)$ and $\chi_l = \chi_l\left(t\right)$, repectively, as the condensate parameters and phase parameters. In princeple, $\phi_l\left(\mathbf{r}\right)$ can be any kind of function. Substituting (6) and (7) into (4)

$$-\hbar f^2\sum_l \dot{\chi}_l\phi_l - \frac{\hbar^2}{2m}f^2\sum_l \chi_l^2\left|\nabla\phi_l\right|^2 - \left(\frac{\hbar^2}{2m}\left|\nabla f\right|^2 + Vf^2 + \frac{g}{2}f^4\right). \tag{8}$$

Using Euler-Lagrange equations for χ_l we obtain

$$\frac{d}{dt}\int d^3\mathbf{r}f^2\phi_l = \frac{\hbar}{m}\int d^3\mathbf{r}f^2\nabla S\cdot\nabla\phi_l \tag{9}$$

which is in fact the continuity equation

$$\int d^3\mathbf{r}\phi_l\left[\frac{\partial f^2}{\partial t} + \nabla\cdot\left(f^2\nabla S\right)\right] = 0. \tag{10}$$

We must choose ϕ_l in such a way that at least one linear combination of ϕ_l gives a good overlapp over $\frac{\partial f^2}{\partial t} + \nabla \cdot (f^2 \nabla S)$, thus enforcing the continuity equation as best as possible. This way phase and density variables become conjugates.

In order to account for the dynamics of all three variational parameter in f therefore we include a variational phase of the form of a polynomial of fourth degree,

$$S(\rho, z, t) = B_\rho(t)\frac{\rho^2}{2} + C(t)\frac{\rho^4}{4} + B_z(t)\frac{z^2}{2}, \tag{11}$$

describing approximately the radial part where $\chi_l = B_\rho, C, B_z$ and $\phi_l = \rho^2/2, \rho^4/4, z^2/2$. This means that the problem in (1) is due to the number of parameter used at density and phase. As the current is connected to the density variation it is necessary that both, density and phase, have the same number of variational parameters. So we have enough parameters to describe the fluctuations on density.

III.   EQUATIONS OF MOTION

Completed the study of phase we have implemented the polynomial phase (11) in our TF-Ansatz which is as follows:

$$\psi(\mathbf{r}, t) = \sqrt{\frac{N}{R_\rho(t)^2 R_z(t) A_0(t)}} \left[\frac{\rho^2}{\rho^2 + \xi(t)^2}\right]^{\frac{\ell}{2}} e^{i\ell\varphi} \sqrt{1 - \frac{\rho^2}{R_\rho(t)^2} - \frac{z^2}{R_z(t)^2}}$$
$$\times \exp\left[iB_\rho(t)\frac{\rho^2}{2} + iC(t)\frac{\rho^4}{4} + iB_z(t)\frac{z^2}{2}\right], \tag{12}$$

where A_0 (All functions $A_i(\alpha)$ are calculated in Appendix B), which is determined by the normalization condition

$$N = \int \psi(\mathbf{r}, t)\, d\mathbf{r}, \tag{13}$$

is a function of $\alpha(t) \equiv \xi(t)/R_\rho(t)$, being $\xi(t)$ the vortex core, $R_\rho(t)$ the radius of the condensate in $\hat{\rho}$ direction and $R_z(t)$ is the condensate radius in axial direction ($\hat{z}$). This wave function has the integration limits determined by $1 - \frac{\rho^2}{R_\rho^2} - \frac{z^2}{R_z^2} \geq 0$, i.e., the wave function is approximately an inverted parabola (TF-shape), unless the central vortex, whose the extension in the region of negative numbers is null. By dealing with a Bose-Einstein condensate which has a density given by a TF-shape, the trapping potential in cylindrical coordinates is described by $V(\rho, z) = \frac{1}{2}m\omega_\rho^2(\rho^2 + \lambda^2 z^2)$ where the anisotropy is $\lambda = \omega_z/\omega_\rho$, that is, for each value of λ the magneto-optical trap (MOT) features different shapes. For λ is equal to unity, the harmonic potential is isotropic. As for $\lambda < 1$ it shows itself as a prolate shape where it is elongated along of $\hat{z}$, and being flatted at the opposite direction when $\lambda > 1$. The shape of trapping potential obviously
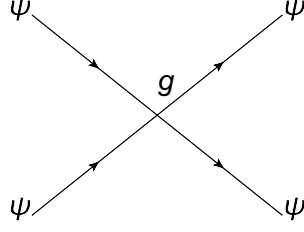
5

Figure 2: Feynman's diagram of the atom-atom interaction in the Bose-Einstein condensates subject.

sets the condensate format. Note that when we sets a value for λ, obligatorily greater than zero, indeed it means that ω_ρ is fixed and we are setting the value of ω_z which eventually determines the shape of the sample.

The atom-atom interaction is $U_{int} = g\,|\psi\,(\mathbf{r},t)|^2$ (Figure 2), whose physical meaning is the scattering in s-wave, i.e., low energy scattering. Because of this, the interaction parameter is proportional to the scattering length a_s, which is $g = 4\pi\hbar^2 a_s/m$.

The Lagrangian density,

$$\mathcal{L} = \mathcal{L}_{time} + \mathcal{L}_{kin} + \mathcal{L}_{pot} + \mathcal{L}_{int}, \tag{14}$$

has four components: temporal, kinetic, potential and interaction potential. Similarly we can split our Lagrangian,

$$L = \int \mathcal{L} d\mathbf{r}. \tag{15}$$

Following this way we have computed all parts of the Lagrangian.

Temporal term:

$$\mathcal{L}_{time} = \frac{i\hbar}{2}\left[\psi^*\,(\mathbf{r},t)\,\frac{\partial\psi\,(\mathbf{r},t)}{\partial t} - \psi\,(\mathbf{r},t)\,\frac{\partial\psi^*\,(\mathbf{r},t)}{\partial t}\right]$$

$$L_{time} = -\frac{N\hbar}{2}\left(D_1\dot{B}_\rho R_\rho^2 + D_2\dot{B}_z R_z^2 + \frac{1}{2}D_3\dot{C}R_\rho^4\right). \tag{16}$$

Kinetic term:

$$\mathcal{L}_{kin} = -\frac{\hbar^2}{2m}\left[\nabla\psi^*\,(\mathbf{r},t)\right]\left[\nabla\psi\,(\mathbf{r},t)\right]$$

$$L_{kin} = -\frac{N\hbar^2}{2m}\left[D_1 B_\rho^2 R_\rho^2 + D_2 B_z^2 R_z^2 + 2D_3 B_\rho C R_\rho^4 + R_\rho^{-2}\left(\ell^2 D_4 + D_5\right) + D_6 C^2 R_\rho^6\right]. \tag{17}$$

Potential term (harmonic trap):

$$\mathcal{L}_{pot} = -\frac{1}{2}m\omega_\rho^2\left(\rho^2 + \lambda^2 z^2\right)\psi^*\,(\mathbf{r},t)\,\psi\,(\mathbf{r},t)$$

$$L_{pot} = -\frac{N}{2}m\omega_\rho^2\left(D_1 R_\rho^2 + \lambda^2 D_2 R_z^2\right). \tag{18}$$

Atom-atom interaction potential term:

$$\mathcal{L}_{int} = -\frac{g}{2}\left[\psi^*\left(\mathbf{r},t\right)\psi\left(\mathbf{r},t\right)\right]^2$$

$$L_{int} = -\frac{N^2 g D_7}{2R_\rho^2 R_z}. \tag{19}$$

The functions of α, D_i, are: $D_i = A_i/A_0$, with exception of $D_7 = A_7/A_0^2$. So the Lagrangian is the sum of each contribution, $L = L_{time} + L_{kin} + L_{pot} + L_{int}$. For simplicity we can scale the parameters of Lagrangian to make them dimensionless, which are the following changes:

$$R_\rho(t) \to a_{osc} r_\rho(t),$$
$$R_z(t) \to a_{osc} r_z(t),$$
$$\xi(t) \to a_{osc} r_\xi(t),$$
$$B_\rho(t) \to a_{osc}^{-2}\beta_\rho(t),$$
$$B_z(t) \to a_{osc}^{-2}\beta_z(t),$$
$$C(t) \to a_{osc}^{-4}\zeta(t)$$

and

$$t \to \omega_\rho^{-1}\tau;$$

where the harmonic oscillator length is $a_{osc} = \sqrt{\hbar/m\omega_\rho}$, and the dimensionless parameter of interaction is $\gamma = Na_s/a_{osc}$. Thus the Lagrangian becomes

$$L = -\frac{N\hbar\omega_\rho}{2}\left[D_1 r_\rho^2\left(\dot{\beta}_\rho + \beta_\rho^2 + 1\right) + D_2 r_z^2\left(\dot{\beta}_z + \beta_z^2 + \lambda^2\right)\right.$$
$$\left. + D_3 r_\rho^4\left(\frac{1}{2}\dot{\zeta} + 2\beta_\rho\zeta\right) + \ell^2 r_\rho^{-2}\left(D_4 + D_5\right) + D_6\zeta^2 r_\rho^6 + D_7\frac{4\pi\gamma}{r_\rho^2 r_z}\right]. \tag{20}$$

Taking the Euler-Lagrange equations,

$$\frac{d}{dt}\left(\frac{\partial L}{\partial\dot{q}_i}\right) - \frac{\partial L}{\partial q_i} = 0, \tag{21}$$

for each one of the six variational parameters from Lagrangian (20) hence six differential equa-

tions:

$$\beta_\rho - \frac{\dot{r}_\rho}{r_\rho} - \frac{D_1'\dot{\alpha}}{2D_1} + \frac{D_3 r_\rho^2 \zeta}{D_1} = 0 \qquad (22)$$

$$\beta_z - \frac{\dot{r}_z}{r_z} - \frac{D_2'\dot{\alpha}}{2D_2} = 0 \qquad (23)$$

$$\zeta - \frac{D_3 \dot{r}_\rho}{D_6 r_\rho} - \frac{D_3 \dot{\alpha}}{4D_6 r_\rho^2} + \frac{D_3 \beta_\rho}{D_6 r_\rho^2} = 0 \qquad (24)$$

$$D_1 r_\rho \left(\dot{\beta}_\rho + \beta_\rho^2 + 1 \right) + D_3 r_\rho^3 \left(\dot{\zeta} + 4\beta_\rho \zeta \right) -$$
$$\frac{\ell^2}{r_\rho^3} (D_4 + D_5) + 3D_6 \zeta^2 r_\rho^5 - D_7 \frac{4\pi\gamma}{r_\rho^3 r_z} = 0 \qquad (25)$$

$$D_2 r_z \left(\dot{\beta}_z + \beta_z^2 + \lambda^2 \right) - D_7 \frac{2\pi\gamma}{r_\rho^2 r_z^2} = 0 \qquad (26)$$

$$D_1' r_\rho^2 \left(\dot{\beta}_\rho + \beta_\rho^2 + 1 \right) + D_2' r_z^2 \left(\dot{\beta}_z + \beta_z^2 + \lambda^2 \right) + D_3' r_\rho^4 \left(\frac{1}{2}\dot{\zeta} + 2\beta_\rho \zeta \right) +$$
$$\frac{\ell^2}{r_\rho^2} (D_4' + D_5') + D_6' \zeta^2 r_\rho^6 - D_7' \frac{4\pi\gamma}{r_\rho^2 r_z} = 0. \qquad (27)$$

Solving the equations for the parameters arising from the phase, which are related with the variation of the curvature of the wave function, we have:

$$\beta_\rho = \frac{\dot{r}_\rho}{r_\rho} + F_1 \dot{\alpha}, \qquad (28)$$

$$\beta_z = \frac{\dot{r}_z}{r_z} + F_2 \dot{\alpha} \qquad (29)$$

and

$$\zeta = F_3 \frac{\dot{\alpha}}{r_\rho^2}; \qquad (30)$$

where

$$F_1 = \frac{D_3' D_3 - 2D_1' D_6}{4 \left(D_3^2 - D_1 D_6 \right)}, \qquad (31)$$

$$F_2 = \frac{D_2'}{2D_2} \qquad (32)$$

and

$$F_3 = \frac{2D_1' D_3 - D_1 D_3'}{4 \left(D_3^2 - D_1 D_6 \right)}. \qquad (33)$$

Replacing (28), (29) and (30) in equations (25), (26) and (27), we reduce our six coupled

equations in only three equations, also coupled, which are given by:

$$D_1 \left(\ddot{r}_\rho + r_\rho \right) + G_1 r_\rho \ddot{\alpha} + G_2 r_\rho \dot{\alpha}^2 + G_3 \dot{r}_\rho \dot{\alpha} - G_4 \frac{\ell^2}{r_\rho^3} - D_7 \frac{4\pi\gamma}{r_\rho^3 r_z} = 0 \qquad (34)$$

$$D_2 \left(\ddot{r}_z + \lambda^2 r_z \right) + G_5 r_z \ddot{\alpha} + G_6 r_z \dot{\alpha}^2 + G_7 \dot{r}_z \dot{\alpha} - D_7 \frac{2\pi\gamma}{r_\rho^2 r_z^2} = 0 \qquad (35)$$

$$D_1' r_\rho \left(\ddot{r}_\rho + r_\rho \right) + D_2' r_z \left(\ddot{r}_z + \lambda^2 r_z \right) + \left(G_8 r_\rho^2 + G_9 r_z^2 \right) \ddot{\alpha} + \left(G_{10} r_\rho^2 + G_{11} r_z^2 \right) \dot{\alpha}^2$$
$$+ \left(G_{12} r_\rho \dot{r}_\rho + G_{13} r_z \dot{r}_z \right) \dot{\alpha} + G_{14} \frac{\ell^2}{r_\rho^2} + D_7' \frac{4\pi\gamma}{r_\rho^2 r_z} = 0, \qquad (36)$$

with

$$G_1 = D_1 F_1 + D_3 F_3 \qquad (37)$$

$$G_2 = D_1 \left(F_1^2 + F_1' \right) + D_3 \left(4F_1 F_3 + F_3' \right) + 3D_6 F_3^2 \qquad (38)$$

$$G_3 = 2 \left(D_1 F_1 + D_3 F_3 \right) = 2G_1 \qquad (39)$$

$$G_4 = D_4 + D_5 \qquad (40)$$

$$G_5 = D_2 F_2 \qquad (41)$$

$$G_6 = D_2 \left(F_2^2 + F_2' \right) \qquad (42)$$

$$G_7 = 2D_2 F_2 = 2G_5 \qquad (43)$$

$$G_8 = D_1' F_1 + \frac{1}{2} D_3' F_3 \qquad (44)$$

$$G_9 = D_2' F_2 \qquad (45)$$

$$G_{10} = D_1' \left(F_1^2 + F_1' \right) + D_3' \left(\frac{1}{2} F_3' + 2F_1 F_3 \right) + D_6' F_3^2 \qquad (46)$$

$$G_{11} = D_2' \left(F_2^2 + F_2' \right) \qquad (47)$$

$$G_{12} = 2D_1' F_1 + D_3' F_3 \qquad (48)$$

$$G_{13} = 2D_2' F_2 = 2G_9 \qquad (49)$$

$$G_{14} = D_4' + D_5'. \qquad (50)$$

The terms $D_1 r_\rho$, $D_2 \lambda^2 r_z$, $D_1' r_\rho^2$ and $D_2' r_z^2$ are responsible for condensate trapping, if they are thrown away we have the free expansion equations. The parameter γ indicates the elements that give the contribution of the atomic interaction potential, while the fractions proportional to r_ρ^{-2} and r_ρ^{-3} are result of the kinetic contribution due to the presence of the vortex with charge ℓ, having the effect of adding a quantum pressure. The remaining factors represent the coupling effect between the radii of the condensate and the vortex core.

Making the velocities ($\dot{r}_\rho$, $\dot{r}_z$ e $\dot{\alpha}$) and accelerations ($\ddot{r}_\rho$, $\ddot{r}_z$ e $\ddot{\alpha}$) equal to zero then we have

the equations for the stationary solution.

$$D_1 \rho_0 = G_4 \frac{\ell^2}{\rho_0^3} + D_7 \frac{4\pi\gamma}{\rho_0^3 z_0} \tag{51}$$

$$D_2 \lambda^2 z_0 = D_7 \frac{2\pi\gamma}{\rho_0^2 z_0^2} \tag{52}$$

$$D_1' \rho_0^2 + D_2' \lambda^2 z_0^2 = -G_{14} \frac{\ell^2}{\rho_0^3} - D_7' \frac{4\pi\gamma}{\rho_0^2 z_0} \tag{53}$$

Remembering that now the α functions become functions of α_0, which is time-independent. We improve the Newton numerical method to solve the coupled stationary equations above. The value of the atomic interaction parameter which will be used is $\gamma = 800$. This value is well close to the experiment value with Rubidium [22].

IV. COLLECTIVE EXCITATIONS

When the vortex is introduced on system it breaks the symmetry of the phase which leads to open a degenerescence onto collective modes of the condensate. Thus we expect to find two modes equivalent to monopole (breathing), and two others equivalent to quadrupole. To obtain from the motion equations a response of the condensate subjected to an external perturbation, we have linearized these equations which is equivalent to calculate the Bogoliubov spectrum. Therefore, we say that the condensate is slightly displaced from its equilibrium position, which in mathematical language is $r_\rho(t) \to \rho_0 + \delta_\rho(t)$, $r_z(t) \to z_0 + \delta_z(t)$ e $\alpha(t) \to \alpha_0 + \delta_\alpha(t)$. Following these changes and neglecting second order terms we have:

$$D_1 \ddot{\delta}_\rho + G_1 \rho_0 \ddot{\delta}_\alpha + \left(D_1 + 3G_4 \frac{\ell^2}{\rho_0^4} + D_7 \frac{12\pi\gamma}{\rho_0^4 z_0} \right) \delta_\rho +$$
$$\left(D_7 \frac{4\pi\gamma}{\rho_0^3 z_0^2} \right) \delta_z + \left(D_1' \rho_0 - G_4' \frac{\ell^2}{\rho_0^3} - D_7' \frac{4\pi\gamma}{\rho_0^3 z_0} \right) \delta_\alpha = 0 \tag{54}$$

$$D_2 \ddot{\delta}_z + G_5 z_0 \ddot{\delta}_\alpha + \left(D_7 \frac{4\pi\gamma}{\rho_0^3 z_0^2} \right) \delta_\rho + \left(D_2 \lambda^2 + D_7 \frac{4\pi\gamma}{\rho_0^2 z_0^3} \right) \delta_z +$$
$$\left(D_2' \lambda^2 z_0 - D_7' \frac{2\pi\gamma}{\rho_0^2 z_0^2} \right) \delta_\alpha = 0 \tag{55}$$

$$D_1' \rho_0 \ddot{\delta}_\rho + D_2' z_0 \ddot{\delta}_z + \left(G_8 \rho_0^2 + G_9 z_0^2 \right) \ddot{\delta}_\alpha + \left(2D_1' \rho_0 - 2G_{14} \frac{\ell^2}{\rho_0^3} - D_7' \frac{8\pi\gamma}{\rho_0^3 z_0} \right) \delta_\rho +$$
$$\left(2D_2' \lambda^2 z_0 - D_7' \frac{4\pi\gamma}{\rho_0^2 z_0^2} \right) \delta_z + \left(D_1'' \rho_0^2 + D_2'' \lambda^2 z_0^2 + G_{14}' \frac{\ell^2}{\rho_0^2} + D_7'' \frac{4\pi\gamma}{\rho_0^2 z_0} \right) \delta_\alpha = 0. \tag{56}$$

The zeroth order terms form the stationary solution, and they vanish. As mentioned in the previous section, the functions of α become functions of α_0 which is time-independent. For
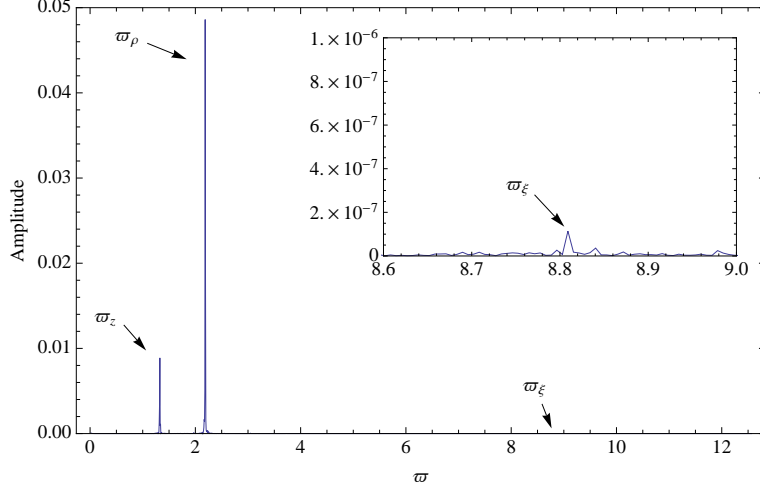
10

Figure 3: Numerical simulations using xmds [23], where we set $\gamma = 800$, $\tilde{\mu} = 20.74$ and $\lambda = 0.9$, and ϖ_i are the frequencies of the oscillation modes, going from less energetic ϖ_z to more energetic ϖ_ξ.

convenience we're changing to the matrix notation,

$$M\ddot{\delta} + V\delta = 0 \tag{57}$$

$$\begin{pmatrix} m_{11} & 0 & m_{13} \\ 0 & m_{22} & m_{23} \\ m_{31} & m_{32} & m_{33} \end{pmatrix} \begin{pmatrix} \ddot{\delta}_\rho \\ \ddot{\delta}_z \\ \ddot{\delta}_\alpha \end{pmatrix} + \begin{pmatrix} v_{11} & v_{12} & v_{13} \\ v_{21} & v_{22} & v_{23} \\ v_{31} & v_{32} & v_{33} \end{pmatrix} \begin{pmatrix} \delta_\rho \\ \delta_z \\ \delta_\alpha \end{pmatrix} = 0. \tag{58}$$

Calculating the dispersion relation,

$$\det\left(M^{-1}V - \varpi^2 I\right) = 0, \tag{59}$$

this results in the frequency of the collective modes of oscillation. The above determinant is a cubic function of ϖ^2, thus

$$-\varpi^6 + b\varpi^4 - c\varpi^2 + d = 0, \tag{60}$$

whose solution is in the Appendix C. Now the determinants $\det M$ and $\det V$ are, both, positive for $\ell = 1$. Meaning that we are in the lower energy state for the case of a central vortex in a Bose-Einstein condensate therefore ϖ^2 shall also be positive, i.e. the frequencies ϖ may not be imaginary. According to this result we have three frequencies ϖ_i $(i = z, \rho, \xi)$ which can not be linked to only a single mode of oscillation, namely we have three frequencies and four modes of oscillation in total, of which only three modes can be observed according to the anisotropy of harmonic potential as it is shown in figure 4. From the four modes, two of them represent the monopolo oscillation, and the other two represent the quadrupole oscillation for the atomic
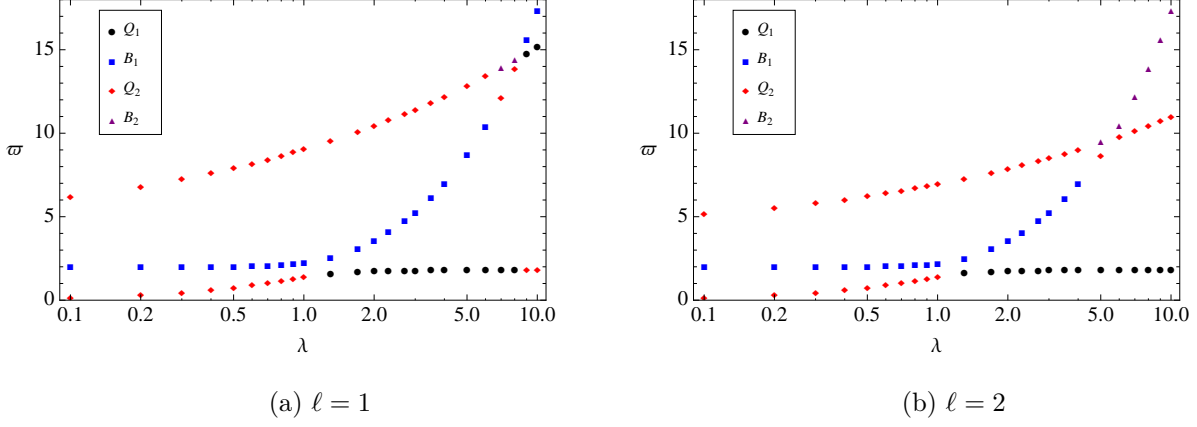
11

(a) $\ell = 1$ (b) $\ell = 2$

Figure 4: The frequencies of oscillation modes of a condensate containing a single vortex at its center.

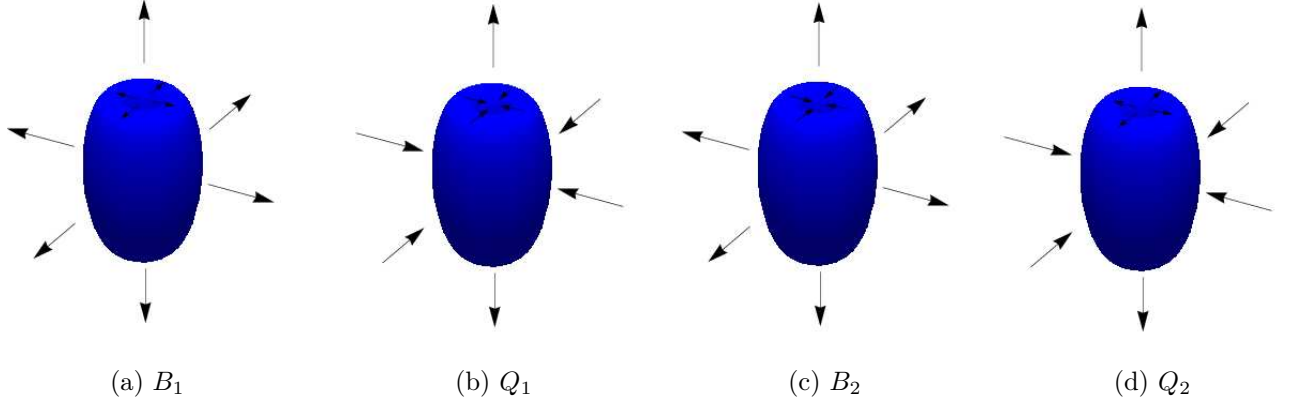(a) B_1 (b) Q_1 (c) B_2 (d) Q_2

Figure 5: A picture drawing which represents the collective modes.

cloud. The first two are when the core of the vortex is in phase with the direction of the radius ρ (B_1 and Q_1 in figures 5a and 5b), and the last two have the core of the vortex in phase with the axial radius (B_2 and Q_2 in figures 5c and 5d). Note that there are points on figure 4 which they look like degenerate modes however they do not. Extrapolating these calculations to an ideal situation where $\gamma = 0$, we decouple the equations of motions. Therefore, the ϖ_z (lower frequency) represents only a R_z oscillation, ϖ_ρ (middle frequency) represents only a R_ρ oscillation and ϖ_ξ (upper frequency) represents only a ξ oscillation.

The numerical simulations was done to validate our results (figure 3), and frequencies values ϖ_i in the variational calculations differ from numerical values by less than 1%.

For $\ell = 1$ (figure 4a), there are two Q_2 it means that the difference between them is on amplitude of oscillation, i.e. the amplitude of vortex code is two order of magnitude lower at the less energetic mode. Indeed, it occurs when $0.1 \leq \lambda \leq 1.3$. At $\lambda = 7$ is the R_ρ radius

which shows itself almost stopped on $\varpi_\rho = 12.144$ (Q_2). The same happens when $\ell = 2$ (figure 4b), the vortex core is almost stopped for the lower frequency in the same interval of λ, and at $\lambda = 4$ is the most energetic mode ($\varpi_\xi = 9.053$) which shows the axial radius almost stopped.

As we increase ℓ, the energy that is necessary to excite the mode with frequency ϖ_ξ will be lower. However, these calculations just can be used when the vortex core is smaller and smaller than the condensates radius, it means that we have to consider the values of λ and γ to know if our approach works. For a giant vortex it is necessary other trial function which has a Gaussian function at the place of the TF-function as background.

V.   MODULATING THE SCATTERING LENGTH

The mechanisms of excitation of collective modes, which were described in the previous section, is via a modulation of scattering length, i.e.

$$a_s(t) = a_0 + \delta a \cos(\Omega t), \tag{61}$$

this is equivalent to do $\gamma \to \gamma(\tau)$ with the same form of $a_s(t)$,

$$\gamma(\tau) = \gamma_0 + \delta\gamma \cos(\Omega\tau). \tag{62}$$

Where γ_0 is the average of the interaction parameter, $\delta\gamma$ is the modulation amplitude and the frequency Ω with which excites the modes.

$$M\ddot{\delta} + V\delta = P\cos(\Omega\tau) \tag{63}$$

with

$$P = 2\pi\delta\gamma \begin{pmatrix} \frac{2D_7}{r_{\rho 0}^3 r_{z0}} \\ \frac{D_7}{r_{\rho 0}^2 r_{z0}^2} \\ \frac{D_7'}{r_{\rho 0}^2 r_{z0}} \end{pmatrix}. \tag{64}$$

We assumed that $\delta\gamma$ is too smaller than others fluctuations, and the particular solution of (63) is

$$\delta(\tau) = \frac{M^{-1}P}{(M^{-1}V - \Omega^2)} \cos(\Omega\tau). \tag{65}$$

In Figure 6 is excited through of non-linear equations the more energetic oscillation to a condensate with anisotropy $\lambda = 0.1$. It can be seen that its oscillation is similar to a beat wave, where it shows the higher frequency ϖ modulated by a cosine wave with frequency Ω close to the resonance.
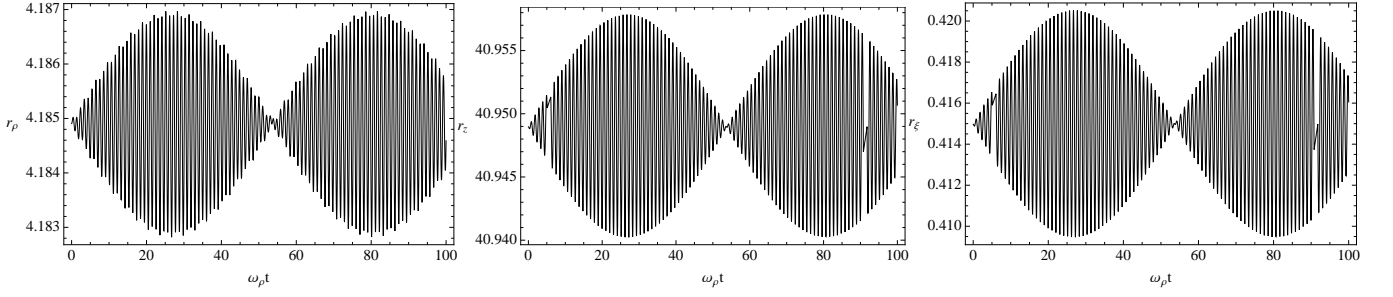
Figure 6: Collective excitation for $\gamma_0 = 800$, $\delta\gamma = 0.4$, $\lambda = 0.1$ e $\Omega = 6$.

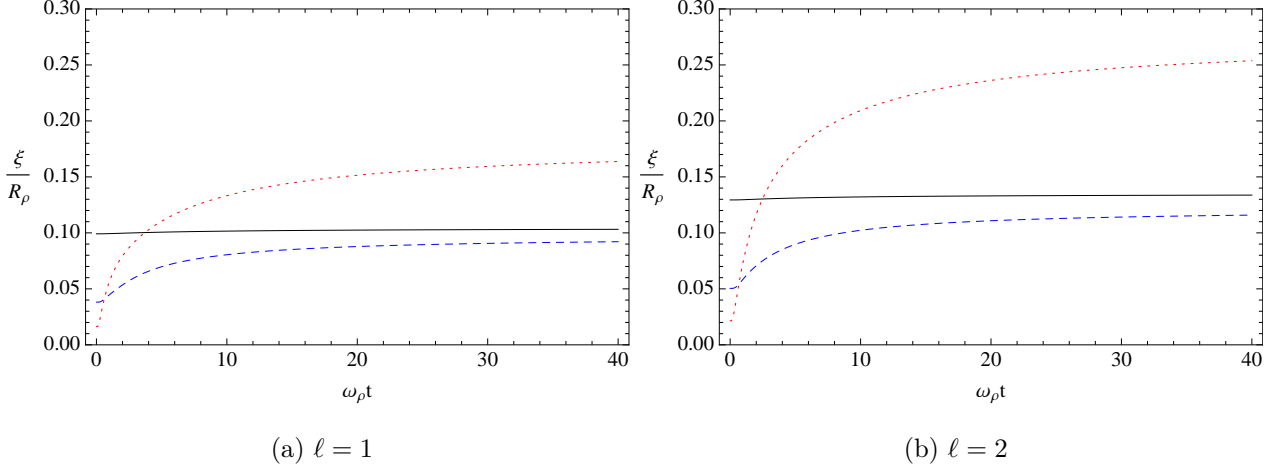(a) $\ell = 1$

(b) $\ell = 2$

Figure 7: This graphic shows the free expansion of the $\alpha(t) = \xi(t)/R_\rho(t)$, being the black line to a prolate condensate ($\lambda = 0.1$), the blue line to the isotropic case ($\lambda = 1$) and the yellow line to a oblate condensate ($\lambda = 8$).

VI.   FREE EXPANSION

The interest in free expansion comes from the fact that we can only make measurements of condensate after switching off the trapping potential. For this purpose, as previously mentioned, simply use the equations of motion ((34), (35) e (36)) without the fraction arising from the harmonic potential, it means

$$D_1\ddot{r}_\rho + G_1 r_\rho \ddot{\alpha} + G_2 r_\rho \dot{\alpha}^2 + G_3 \dot{r}_\rho \dot{\alpha} - \frac{G_4}{r_\rho^3} - \frac{4D_7\gamma}{r_\rho^3 r_z} = 0 \tag{66}$$

$$D_2\ddot{r}_z + G_5 r_z \ddot{\alpha} + G_6 r_z \dot{\alpha}^2 + G_7 \dot{r}_z \dot{\alpha} - \frac{2D_7\gamma}{r_\rho^2 r_z^2} = 0 \tag{67}$$

$$D_1' r_\rho \ddot{r}_\rho + D_2' r_z \ddot{r}_z + \left(G_8 r_\rho^2 + G_9 r_z^2\right)\ddot{\alpha} + \left(G_{10} r_\rho^2 + G_{11} r_z^2\right)\dot{\alpha}^2$$
$$+ \left(G_{12} r_\rho \dot{r}_\rho + G_{13} r_z \dot{r}_z\right)\dot{\alpha} + \frac{G_{14}}{r_\rho^3} + \frac{4D_7'\gamma}{r_\rho^2 r_z} = 0, \tag{68}$$

whose initial conditions are given by the stationary solution. This result agrees with our preview

14

work [21], where the free expansion of the vortex core is given on figure 7. In the work that preceding the present one[21], the figure 7b could not be calculated.

VII. CONCLUSIONS

In this paper we proposed a change in the phase used the variational method to correct the imaginary frequencies of collective modes when we have a parameter that describes the dynamics of the vortex core. This change was that we had a proper atomic density fluctuation.

Based on the continuity equation, we conclude that we have a variational phase parameter, respectively, for each parameter in density. With that in calculating the frequencies for the vortex with charge $\ell = 1$, they gave them real. Thus it was observed that the vortex opens a degeneracy in the collective modes, which depends on the anisotropy of the trap and the atomic interaction parameter. This degeneration is linked to the oscillation of the vortex core, which needs a lot of energy to dephase its oscillation with respect to the radial component of the atomic cloud.

With modulation of scattering length we show that these new modes can be excited.

We also made the free expansion of this system, which can evaluate the core of the vortex to $\ell \geq 2$, in contrast previous work which only allowed us to calculate the free expansion of this core vortex radius when $\ell = 1$. We maintain, with this Ansatz, the logarithmic ratio of the energy vortex.

Appendix A: Two Thomas-Fermi approaches for the profile containing a single vortex

Two approaches to the density profile can be obtained from the GPE when there is a singularity at the center of the condensate. First we write the time-independent GPE in cylindrical coordinates,

$$\mu\psi\left(\rho,z\right) = -\frac{\hbar^2}{2m}\nabla^2_{\rho,z}\psi\left(\rho,z\right) + \frac{\hbar^2\ell^2}{2m\rho^2}\psi\left(\rho,z\right) + V\left(\rho,z\right)\psi\left(\rho,z\right) + g\left|\psi\left(\rho,z\right)\right|^2\psi\left(\rho,z\right), \quad \text{(A1)}$$

where $\nabla^2_{\rho,z}$ is the laplacian just for ρ and z coordinates. Consider then the effective potential much greater than the kinetic energy for a harmonic and isotropic trap,

$$\mu = \frac{\hbar^2\ell^2}{2m\rho^2} + \frac{1}{2}m\omega^2_\rho\left(\rho^2 + \lambda^2 z^2\right) + gn\left(\rho,z\right), \quad \text{(A2)}$$

being $n\left(\rho,z\right) = \left|\psi\left(\rho,z\right)\right|^2$. There is two ways to follow. The fist one is the most usual, and it

consists in isolate $n(\rho, z)$ that gives

$$n(\rho, z) = \frac{\mu}{g} \left(1 - \frac{\xi^2}{\rho^2} - \frac{\rho^2}{R_\rho^2} - \frac{z^2}{R_z^2} \right) \Theta \left(1 - \frac{\xi^2}{\rho^2} - \frac{\rho^2}{R_\rho^2} - \frac{z^2}{R_z^2} \right),$$ (A3)

with Θ being the step function, and the radii of TF are:

$$R_\rho = \sqrt{\frac{2\mu}{m\omega_\rho^2}}, \ R_z = \sqrt{\frac{2\mu}{m\lambda^2\omega_\rho^2}} \text{ and } \xi = \sqrt{\frac{\hbar^2\ell^2}{2m\mu}}.$$ (A4)

Now the wave function must have the phase $\ell\varphi$,

$$\psi(\rho, \varphi, z) = e^{i\ell\varphi} \left(\frac{\mu}{g} \right)^{\frac{1}{2}} \sqrt{1 - \frac{\xi^2}{\rho^2} - \frac{\rho^2}{R_\rho^2} - \frac{z^2}{R_z^2}},$$ (A5)

and its limits is described for this region of space: $1 - \frac{\xi^2}{\rho 2} - \frac{\rho^2}{R_\rho^2} - \frac{z^2}{R_z^2} \geq 0$.

The second approach is similar, nevertheless it is fairly simple to work when we are considering of a condensate in three dimensions. In (A2) we use relation of the healing length,

$$\frac{\hbar^2\ell^2}{2m\xi^2} = gn(\rho, z),$$ (A6)

rendering it follows:

$$\mu = \frac{1}{2}m\omega_\rho^2 \left(\rho^2 + \lambda^2 z^2 \right) + \left(\frac{\xi^2}{\rho^2} + 1 \right) gn(\rho, z).$$ (A7)

Now we have isolated the density $n(\rho, z)$, thus

$$n(\rho, z) = \frac{\mu}{g} \left(\frac{\rho^2}{\rho^2 + \xi^2} \right) \left(1 - \frac{\rho^2}{R_\rho^2} - \frac{z^2}{R_z^2} \right) \Theta \left(1 - \frac{\rho^2}{R_\rho^2} - \frac{z^2}{R_z^2} \right),$$ (A8)

where the radii are given as the previous ones, except by the vortex core size which does not depend on μ. In this description the vortex core size is associated with the interaction parameter g, and it may vary with the ratio μ/g. The same phase has to be added when we use the wave function. The second advantage of this second way of wringing a TF-density profile is the fact that we can separate the density of vortex from the back ground density[19]. We shall call

$$n_{TF}(\rho, z) = \frac{\mu}{g} \left(1 - \frac{\rho^2}{R_\rho^2} - \frac{z^2}{R_z^2} \right) \Theta \left(1 - \frac{\rho^2}{R_\rho^2} - \frac{z^2}{R_z^2} \right)$$ (A9)

and now follows

$$\begin{aligned} n(\rho, z) &= \left(\frac{\rho^2}{\rho^2 + \xi^2} \right) n_{TF}(\rho, z) \\ &= \left(1 - \frac{\xi^2}{\rho^2 + \xi^2} \right) n_{TF}(\rho, z) \\ &= n_{bg}(\rho, z) + n_v(\rho, z), \end{aligned}$$ (A10)

where $n_{bg}(\rho, z) = n_{TF}(\rho, z)$ e

$$n_v(\rho, z) = \left(-\frac{\xi^2}{\rho^2 + \xi^2} \right) n_{TF}(\rho, z).$$ (A11)

The difference between the energies calculated by both approaches is less than 1%.

Appendix B: Functions $A_i(\alpha)$

The functions A_i are results after the TF-functions are integrated, being each one related to one part of the Lagrangian except A_0 which arising from the normalization condition (13). Starting with this one which is more detailed since the procedure is the same for the others mentioned. Doing $\rho \to \rho R_\rho$ and $z \to z R_z$, the normalization integral is

$$A_0(\alpha) = 2\pi \int \int \left(\frac{\rho^2}{\rho^2 + \alpha^2} \right)^\ell \left(1 - \rho^2 - z^2\right) \rho \, d\rho \, dz. \tag{B1}$$

By changing the variables from cylindrical coordinates to spherical coordinates, $\rho = r \sin\theta$ and $z = r \cos\theta$, the limit of integration is simplified.

$$
\begin{aligned}
A_0(\alpha) =& 2\pi \int_0^\pi \int_0^1 \left(\frac{r^2 \sin^2\theta}{r^2 \sin^2\theta + \alpha^2} \right)^\ell \left(1 - r^2\right) r^2 \sin\theta \, dr \, d\theta \\
=& \frac{2\pi^{3/2} (\ell)!}{15 \alpha^{2\ell} \left(\frac{3}{2} + \ell\right)!} \left[\left(3 + 2\ell\alpha^2\right) {}_2F_1 \left(\ell, 1 + \ell; \frac{5}{2} + \ell; -\frac{1}{\alpha^2} \right) \right. \\
& \left. - 2\ell \left(1 + \alpha^2\right) {}_2F_1 \left(1 + \ell, 1 + \ell; \frac{5}{2} + \ell; -\frac{1}{\alpha^2} \right) \right].
\end{aligned}
\tag{B2}
$$

The $_pF_q\left(a_1,\ldots,a_p;b_1,\ldots,b_q;x\right)$ are the hypergeometric functions. Proceeding, the next A_i are:

$$
\begin{aligned}
A_1\left(\alpha\right) =&2\pi\int_0^\pi\int_0^1 r^2\sin^2\theta\left(\frac{r^2\sin^2\theta}{r^2\sin^2\theta+\alpha^2}\right)^\ell\left(1-r^2\right)r^2\sin\theta drd\theta\\
=&\frac{2\pi^{3/2}\left(1+\ell\right)!}{21\alpha^{2\ell}\left(\frac{5}{2}+\ell\right)!}\left[\left(3+2\ell\alpha^2\right){}_2F_1\left(\ell,2+\ell;\frac{7}{2}+\ell;-\frac{1}{\alpha^2}\right)\right.\\
&\left.-2\ell\left(1+\alpha^2\right){}_2F_1\left(1+\ell,2+\ell;\frac{7}{2}+\ell;-\frac{1}{\alpha^2}\right)\right]
\end{aligned}
\tag{B3}
$$

$$
\begin{aligned}
A_2\left(\alpha\right) =&2\pi\int_0^\pi\int_0^1 r^2\cos^2\theta\left(\frac{r^2\sin^2\theta}{r^2\sin^2\theta+\alpha^2}\right)^\ell\left(1-r^2\right)r^2\sin\theta drd\theta\\
=&\frac{\pi^{3/2}\left(\ell\right)!}{4\alpha^{2\ell}\left(\frac{7}{2}+\ell\right)!}\left[\left(7+2\ell\right){}_2F_1\left(\ell,1+\ell;\frac{7}{2}+\ell;-\frac{1}{\alpha^2}\right)\right.\\
&\left.-\left(5+2\ell\right){}_3F_2\left(\ell,1+\ell,\frac{7}{2}+\ell;\frac{5}{2}+\ell,\frac{9}{2}+\ell;-\frac{1}{\alpha^2}\right)\right]
\end{aligned}
\tag{B4}
$$

$$
\begin{aligned}
A_3\left(\alpha\right) =&2\pi\int_0^\pi\int_0^1 r^4\sin^4\theta\left(\frac{r^2\sin^2\theta}{r^2\sin^2\theta+\alpha^2}\right)^\ell\left(1-r^2\right)r^2\sin\theta drd\theta\\
=&\frac{2\pi^{3/2}\left(2+\ell\right)!}{27\alpha^{2\ell}\left(\frac{7}{2}+\ell\right)!}\left[\left(3+2\ell\right){}_2F_1\left(\ell,3+\ell;\frac{9}{2}+\ell;-\frac{1}{\alpha^2}\right)\right.\\
&\left.-2\ell\left(1+\alpha^2\right){}_2F_1\left(1+\ell,3+\ell;\frac{9}{2}+\ell;-\frac{1}{\alpha^2}\right)\right]
\end{aligned}
\tag{B5}
$$

$$
\begin{aligned}
A_4\left(\alpha\right) =&2\pi\int_0^\pi\int_0^1\left(\frac{\alpha^2}{r^2\sin^2\theta+\alpha^2}\right)^2\left(\frac{r^2\sin^2\theta}{r^2\sin^2\theta+\alpha^2}\right)^\ell\left(1-r^2\right)r^2\sin\theta drd\theta\\
=&\frac{2\pi^{3/2}\left(\ell-1\right)!}{3\alpha^{2\ell}\left(\frac{1}{2}+\ell\right)!}\left[\left(1-2\ell\alpha^2\right){}_2F_1\left(\ell,2+\ell;\frac{3}{2}+\ell;-\frac{1}{\alpha^2}\right)\right.\\
&\left.+2\ell\left(1+\alpha^2\right){}_2F_1\left(1+\ell,2+\ell;\frac{3}{2}+\ell;-\frac{1}{\alpha^2}\right)\right]
\end{aligned}
\tag{B6}
$$

$$
\begin{aligned}
A_5\left(\alpha\right) =&2\pi\int_0^\pi\int_0^1\left(\frac{1}{r^2\sin^2\theta}\right)\left(\frac{r^2\sin^2\theta}{r^2\sin^2\theta+\alpha^2}\right)^\ell\left(1-r^2\right)r^2\sin\theta drd\theta\\
=&\frac{2\pi^{3/2}\left(\ell-1\right)!}{9\alpha^{2\ell}\left(\frac{1}{2}+\ell\right)!}\left[\left(3+2\ell\alpha^2\right){}_2F_1\left(\ell,\ell;\frac{3}{2}+\ell;-\alpha^2\right)\right.\\
&\left.-2\ell\left(1+\alpha^2\right){}_2F_1\left(\ell,1+\ell;\frac{3}{2}+\ell;-\frac{1}{\alpha^2}\right)\right]
\end{aligned}
\tag{B7}
$$

$$
\begin{aligned}
A_6\left(\alpha\right) =&2\pi\int_0^\pi\int_0^1 r^6\sin^6\theta\left(\frac{r^2\sin^2\theta}{r^2\sin^2\theta+\alpha^2}\right)^\ell\left(1-r^2\right)r^2\sin\theta drd\theta\\
=&\frac{2\pi^{3/2}\left(3+\ell\right)!}{33\alpha^{2\ell}\left(\frac{9}{2}+\ell\right)!}\left[\left(3+2\ell\alpha^2\right){}_2F_1\left(\ell,4+\ell;\frac{11}{2}+\ell;-\frac{1}{\alpha^2}\right)\right.\\
&\left.-2\ell\left(1+\alpha^2\right){}_2F_1\left(1+\ell,4+\ell;\frac{11}{2}+\ell;-\frac{1}{\alpha^2}\right)\right]
\end{aligned}
\tag{B8}
$$

$$
\begin{aligned}
A_7\left(\alpha\right) =&2\pi\int_0^\pi\int_0^1\left(\frac{r^2\sin^2\theta}{r^2\sin^2\theta+\alpha^2}\right)^2\left(1-r^2\right)^2 r^2\sin\theta drd\theta\\
=&\frac{2\pi^{3/2}\left(2\ell\right)!}{\alpha^{4\ell}\left(\frac{7}{2}+\ell\right)!}{}_2F_1\left(2\ell,1+2\ell;\frac{9}{2}+2\ell;-\frac{1}{\alpha^2}\right).
\end{aligned}
\tag{B9}
$$

Acknowledgments

[1] POLLACK, S. E. et al. Collective excitation of a bose-einstein condensate by modulation of the atomic scattering length. *Physical Review A*, v. 81, n. 5, p. 053627, 2010.

[2] STRINGARI, S. Collective excitation of a trapped bose-einstein-condensad gas. *Physical Review Letters*, v. 77, n. 12, p. 2360, September 1996.

[3] PÉREZ-GARCÍA, V. M. et al. Low energy excitations of a bose-einstein condensate: a time-dependent variational analysis. *Physical Review Letters*, v. 77, n. 27, p. 5320–5323, December 1996.

[4] DALFOVO, F. et al. Theory of bose-einstein condensate in trapped gases. *Reviews of Modern Physics*, v. 71, n. 3, p. 463–512, April 1999.

[5] COURTEILLE, P. W.; BAGNATO, V. S.; YUKALOV, V. I. Bose-einstein condensation of trapped atomic gases. *Laser Physics*, v. 11, n. 6, p. 659–800, 2001.

[6] BUSCH, T. et al. Stability and collective excitations of a two-component bose-einstein condensad gas: A moment approach. *Physical Review A*, v. 56, n. 4, p. 2978, October 1997.

[7] ZHANG, Z.; LIU, W. V. Finite-temperature damping of collective modes of a bcs-bec crossover superfluid. *Physical Review A*, v. 83, n. 2, p. 023617, 2011.

[8] HEISELBERG, H. Collective modes of trapped gases at the bec-bcs crossover. *Physical Review Letters*, v. 93, n. 4, p. 040402, July 2004.

[9] ALTMEYER, A. et al. Precision measurements of collective oscillations in the bec-bsc crossover. *Physical Review Letters*, v. 98, n. 4, p. 040401, January 2007.

[10] ČLOVEČKO, M. et al. New non-goldstone collective mode of bec of magnons in superfluid 3he-b. *Physical Review Letters*, v. 100, n. 15, p. 155301, April 2008.

[11] PETHICK, C. J.; SMITH, H. *Bose-einstein condensation in dilute gases*. 2nd. ed. Cambridge: Cambridge University Press, 2008.

[12] PITAEVSKII, L. P.; STRINGARI, S. *Bose-Einstein Condensation*. First edition. [S.l.]: Oxford University Press Inc, 2003.

[13] SVIDZINSKY, A. A.; FETTER, A. L. Dynamics of a vortex in a trapped bose-einstein condensate. *Physical Review A*, v. 62, p. 063617, November 2000.

[14] SVIDZINSKY, A. A.; FETTER, A. L. Stability of a vortex in a trapped bose-einstein condensate. *Physical Review Letters*, v. 84, n. 26, p. 5919–5923, 2000.

[15] LINN, M.; FETTER, A. L. Small-amplitude normal modes of a vortex in a trapped bose-einstein condensate. *Physical Review A*, v. 61, p. 063603, May 2000.

[16] PÉREZ-GARCÍA, V. M.; GARCÍA-RIPOLL, J. J. Two-mode theory of vortex stability in multi-

component bose-einstein condensates. *Physical Review A*, v. 62, p. 033601, August 2000.

[17] PÉREZ-GARCÍA, V. M. et al. Dynamics of bose-einstein condensates: variational solutions of the gross-pitaevskii equations. *Physical Review A*, v. 56, n. 2, p. 1424–1432, August 1997.

[18] SVIDZINSKY, A. A.; FETTER, A. L. Normal modes of a vortex in a trapped bose-einstein condensate. *Physical Review A*, v. 58, n. 4, p. 3168, October 1998.

[19] O'DELL, D. H. J.; EBERLEIN, C. Vortex in a trapped bose-einstein condensate with dipole-dipole interactions. *Physical Review A*, v. 75, n. 1, p. 013604, 2007.

[20] DALFOVO, F.; MODUGNO, M. Free expansion of bose-einstein condensates with quantized vortices. *Physical Review A*, v. 61, n. 2, p. 023605, January 2000.

[21] TELES, R. P. et al. Free expansion of bose-einstein condensates with a multicharged vortex. *Physical Review A*, v. 87, n. 3, p. 033622, March 2013.

[22] HENN, E. A. de L. *Produção experimental de excitações topológicas em um condensado de Bose-Einstein. 2008. 129p.* Tese (Doutorado) — Instituto de Física de São Carlos, Universidade de São Paulo, São Carlos, 2008.

[23] DENNIS, G. R.; HOPE, J. J.; JOHNSSON, M. T. Xmds2: Fast, scalable simulation of coupled stochastic partial differential equations. *Computer Physics Communications*, v. 184, n. 1, p. 201–208, January 2013.